

Dottorato di Ricerca in Fisica XXXI ciclo

Dottoranda: Marilena Giglio

Titolo progetto di ricerca: **TECNICHE SPETTROSCOPICHE INNOVATIVE PER LA RIVELAZIONE DI TRACCE GASSOSE**

Tutor: Prof. Vincenzo Spagnolo

Third year PhD report

Among mid-IR spectroscopic techniques, Quartz-Enhanced Photoacoustic Spectroscopy (QEPAS) has been demonstrated as one of the most selective, sensitive, compact, robust and low-cost techniques for trace gas optical detection. In QEPAS, a high quality-factor quartz tuning fork (QTF) is used as a sharp resonator to convert acoustic waves generated by the non-radiative relaxation of the target gas absorbing radiation into an electric signal as a result of quartz piezoelectricity. QEPAS does not require bulky optics: a lens is used to focus the laser beam between the two prongs of the QTF. In contrast to other optical detection techniques, QEPAS does not require any optical detector since the QTF itself acts as a detector. The QTF responsivity is wavelength independent, furthermore, the optical alignment is easier and more resilient against imperfect spatial beam quality when the tuning fork is properly designed.

During the third year of the PhD, a new set of custom QTFs with optimized geometry for QEPAS sensing has been designed, fabricated and tested as well as a custom QTF with an electrodes pattern optimizing the first overtone flexural mode charge collection.

The research activity has been also focused on the design, realization and characterization of QEPAS gas sensors employing either standard or custom QTFs, in order to target:

- ethylene at sub-ppm concentrations;
- methane, ethane and propane by employing a single laser source;
- two broad absorption bands of nitrous oxide and several methane absorption features in a 150 cm^{-1} -wide spectral range.

Quartz tuning forks with optimized geometries for QEPAS

Since its introduction in 2002, standard low-cost quartz tuning forks (QTFs) with resonance frequencies at 32.7 kHz are typically employed in QEPAS sensors. The QTF is typically coupled with a pair of tubes, acting as an organ pipe resonator to probe the sound wave. The acoustic detection module composed of the QTF and micro-resonator tubes constitutes the QEPAS spectrophone, which is the core of any QEPAS sensor. Starting in 2013, custom QTFs have been realized in QEPAS sensors following the following two guidelines: i) reduction of the QTF fundamental resonance frequency, for an efficient sound wave generation when targeting slow relaxing gases, ii) increase the prongs spacing in order to facilitate the optical alignments and minimize the photo-thermal noise level. The straightforward approach to design QTFs optimized for QEPAS sensing is to reduce the resonance frequency while keeping high the quality factor. Based on the results obtained during the first PhD year, it has been developed a MATLAB-based software to relate the QTF quality factor and its resonance frequency to its prongs geometries. For each fixed prong geometry (T-prong width, L-prong length), the software calculates the resonance frequency and the related Q-factor, and plots ordered points on the x- (frequencies,

f) and γ - (Q-factors) axis of the coordinate plane. By ranging L from 3 mm to 20 mm and T from 0.2 mm to 3.0 mm, while keeping at a fixed crystal thickness $w = 0.25$ mm value, the calculated ordered points (Q, f) are shown in Fig. 1.

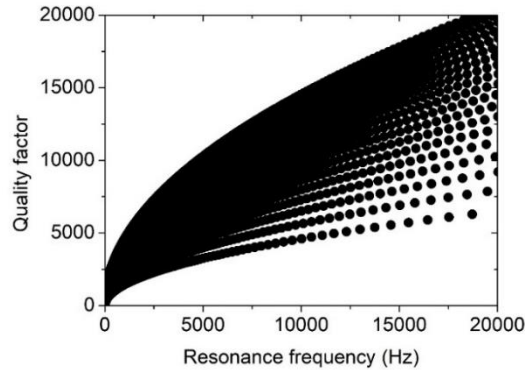


Fig. 1. Q-factor values plotted as a function of the resonance frequency for different prong lengths and thicknesses of quartz tuning fork of crystal width $w = 0.25$ mm, at atmospheric pressure.

At $f = 16$ kHz, one half of the resonance frequency of the standard QTF, L and T values (with $w = 0.25$ mm, which is a standard for quartz wafers) maximizing the quality factor (18,000) are 9.4 mm and 2.0 mm, respectively. In a first step, starting with this prong geometry it has been designed two QTFs differing only in the prong spacing: QTF-S08 having a prong spacing of 0.8 mm, and QTF-S15 with a prong spacing of 1.5 mm. Starting from QTF-S08, a modified geometry for QTF prongs is proposed, in which the prong thickness T is not constant along the prong axis. The thickness function $T(x)$ of the prong is thought out to be a piecewise function that can be written as:

$$T(x) = \begin{cases} T_1 & x \in [0, L_0] \\ T_2 & x \in [L_0, L_1] \end{cases} \quad (1)$$

This prong geometry will be referred as a T-shaped prong and the fork will be indicated as QTF-S08-T. To keep the electrical resistance low, the coupling between the electrodes and the resonance mode must be optimized. This can be achieved by carving rectangular grooves on both surfaces of each prong of QTF-S08. This QTF will be referred to as QTF-S08-G. The set of QTFs is shown in Fig. 2.

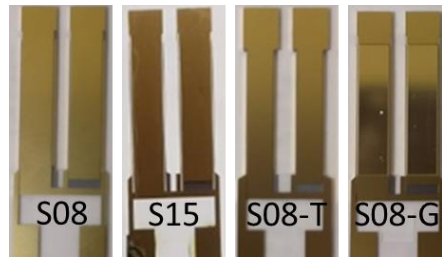


Fig. 2. Picture of the set of custom QTFs

This set of custom QTFs was characterized electrically, in order to determine their resonance properties. Then, the investigated QTF samples were implemented in a QEPAS setup to test their photoacoustic response. The QTF-S08-T provided the best performance in terms of signal-to-noise ratio (SNR=21) and was acoustically coupled with a couple of tubes having an optimized length of 12.4 mm and internal diameter of 1.59 mm, both positioned 200 μm distant from the

QTF. In Fig. 3 the comparison between the water QEPAS signal acquired with the bare QTF-S08-T (dashed red line) and with a spectrophone composed by QTF-S08-T and the tubes is reported.

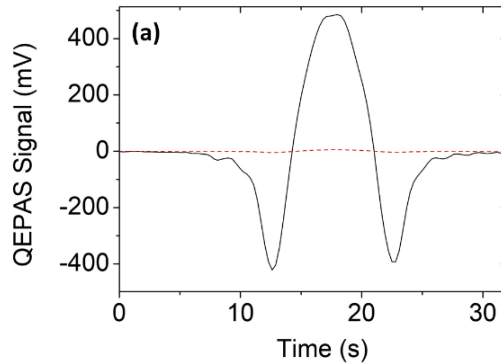


Fig. 3 QEPAS spectral scan of water absorption line acquired with the bare QTF-S08-T (dashed red line) and with a spectrophone composed by QTF-S08-T and a pair of micro-resonator tubes (solid black line).

By employing such a dual-tube micro-resonator system, a SNR enhancement of 60 times was obtained, which represents a record for mid-IR QEPAS systems.

Octupole electrode pattern for tuning forks vibrating at the 1st overtone mode in quartz-enhanced photoacoustic spectroscopy

Custom QTFs, as some of the ones designed and fabricated during the first year, designed to operate with fundamental flexural resonance mode frequency of a few kHz have initiated the implementation of the first overtone flexural modes for QEPAS sensing. In all QEPAS systems demonstrated so far, the electrodes layout of the employed QTFs had a quadrupole pattern, matching the charge distribution generated by the in-plane fundamental mode vibration. Such electrode configuration partially impedes the excitation of the first overtone flexural mode since it should exhibit a different piezoelectric charge distribution. It has been proposed an innovative electrode pattern optimizing the first overtone flexural mode charge collection by analysing the stress field distribution along the QTF prongs. The proposed electrode pattern has an octupole configuration, according to the change of the polarity along the prongs at the zero-stress point occurring for the first overtone vibrational mode. To provide a comparison between quadrupole and octupole electrode configurations in terms of QEPAS sensing performance, both contact patterns have been deposited on two QTFs having the same geometry and size, which were implemented into a sensor system for water vapor trace detection. The two QTFs will be referred as QTF-Q (quadrupole configuration) and QTF-O (octupole configuration), respectively, and the schematic of the two employed electrodes patterns are showed in Fig. 4.

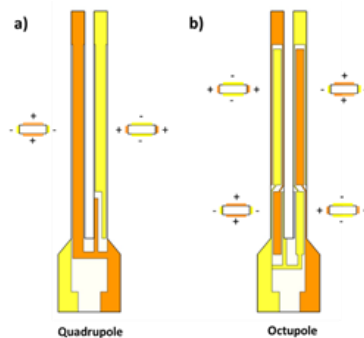


Fig. 4 Schematic of the QTF-Q with a quadrupole electrode pattern (a) and of the QTF-O having an octupole electrode pattern (b). The pattern configuration is inverted in the QTFs back surfaces. The small rectangles represent sections of the prong with the corresponding charge distributions.

The influence of the electrode layout on the main QTFs characteristics, namely the resonance frequency, the quality factor and the electrical resistance were investigated. The obtained parameters are listed in Table I.

Table I Resonance frequency, quality factor and electrical resistance values measured for the QTF-Q when vibrating at the fundamental or the first overtone mode and for the QTF-O when vibrating at the first overtone mode.

	QTF-Q	QTF-Q	QTF-O
	Fund. mode	Overt. mode	Overt. Mode
Frequency (Hz)	2870.99	17747.47	17834.79
Quality factor	5850	14500	15290
Resistance (k Ω)	810.8	157.6	36.1

Although the quadrupole electrode structure is designed to enhance the excitation of the fundamental mode of the QTF, it is also able to excite the first overtone mode, whereas in QTF-O the fundamental mode is completely suppressed. The Q-factor for both QTFs vibrating at the overtone mode remains almost the same, because the quality factor is mainly affected by loss mechanisms occurring in the vibrating prongs and not by the charge collection efficiency. The implementation of an octupole contact pattern strongly reduces the electrical resistance for the first overtone mode, demonstrating that this configuration collects the charges generated by the prongs oscillations more efficiently.

Both QTFs have been implemented in a QEPAS setup, targeting a water vapor absorption line falling at 1931.76 cm^{-1} , having a line-strength of $3.2 \cdot 10^{-22} \text{ cm/molecule}$. The QEPAS spectral scans of the selected water absorption line obtained for each vibrational mode of the investigated QTFs are shown in Fig. 5.

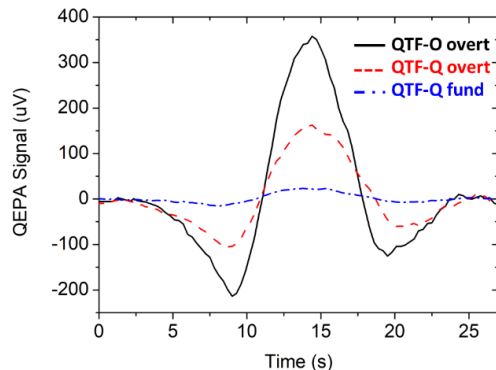


Fig. 5. QEPAS spectral scans of the water absorption line measured with the QTF-O operating at the first overtone mode (solid black curve) and the QTF-Q operating at the fundamental (dot-dashed blue curve) or the overtone (dashed red curve) mode.

The QEPAS spectra show that the peak value measured for QTF-O operating at the overtone mode is ~ 2.3 times higher than that obtained with QTF-Q operating at the overtone mode and ~ 15.3 times higher when QTF-Q operated at the fundamental mode.

Improved quartz-enhanced photoacoustic sensor for sub-ppm ethylene detection employing a new custom QTF

During the second PhD year it has been exploited the QEPAS technique for the detection and the quantification of ethylene, realizing a compact Thorlabs parts-based QEPAS system. During the third year an improved QEPAS-based sensor for ethylene detection was developed, by employing a new custom QTF: QTF-S08-T. The targeted ethylene absorption line falls at 966.38 cm^{-1} with a line strength of $2.2 \cdot 10^{-20} \text{ cm/mol}$. The optical power focused between the QTF prongs was 74 mW. At 120 Torr, with a certified concentration of 100 ppm in N_2 , it has been measured a signal of 615.82 mV and a noise of 0.180 mV, with an integration time of 100ms, leading to a signal-to-noise ratio (SNR) of 3420, corresponding to a minimum detection limit of 29 ppb. Compared with the results previously obtained, by employing a spectrophone composed by QTF-S08-T and two micro-resonator tubes, the achieved MDL was improved by a factor ~ 3.4 . By means of Allan deviation analysis, it has been estimated a noise reduction down to 0.063mV when using an integration time of 10 s, with an ultimate detection limit of 10 ppb, 3 times better than that reached for the previous version of the QEPAS-based ethylene detector. The Allan deviation plot is shown in Fig. 6.

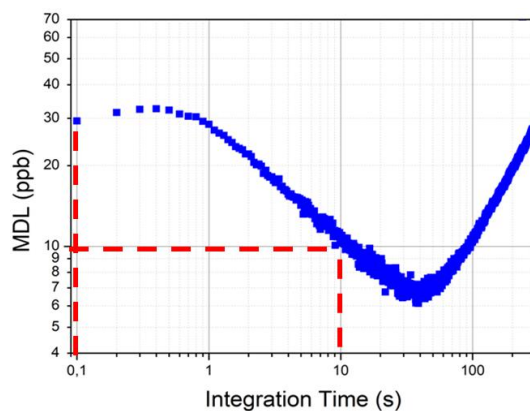


Fig. 6: Allan deviation plot reporting the minimum detection limit achievable by using 100 ms and 10 s integration time.

It has been also calibrated the sensor by acquiring the QEPAS signal corresponding to different ethylene concentrations, obtained by diluting the certified 100 ppm concentration.

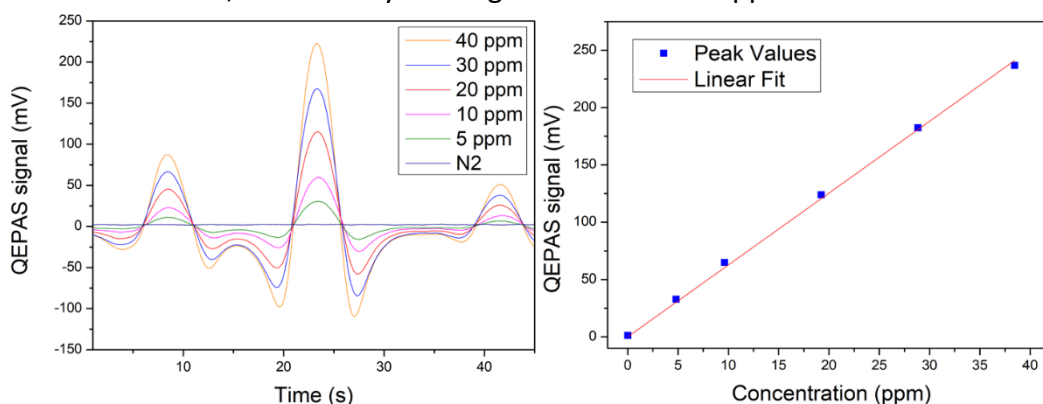


Fig. 7: Spectral scans of ethylene at different concentrations (a) and calibration curve obtained by fitting the peak values measured from the spectral scans (b).

The obtained spectral scans are reported in Fig. 7 (a). From the calibration curve reported in Fig. 7 (b), a QEPAS signal variation of 6.27 mV per ppm was calculated.

Methane, ethane and propane detection using a compact quartz enhanced photoacoustic sensor and a single interband cascade laser

For the petrochemical industry, the monitoring of hydrocarbons such as methane (CH_4 -C1), ethane (C_2H_6 -C2) and propane (C_3H_8 -C3) represents one of the most efficient ways to predict production outputs, estimate reserves and assess raw material quality of source rocks and reservoirs. It has been developed a compact QEPAS sensor prototype for trace gas detection of the three mentioned hydrocarbons by using a single ICL source operating in the spectral range 3.342-3.349 μm .

It has been investigated the full ICL dynamic range to retrieve the most convenient experimental conditions for C1-C2 detection in the current scan mode. Then, it has been determined the best operating conditions in terms of gas pressure and modulation depth and performed a sensor calibration for C1 and C2 detection, by recording the 2f-signal peak signals at different C1 and C2 concentrations, in the range 4-1000ppm and 2-100ppm, respectively. Based on the calibration

results, it has been performed measurements on C1/C2 mixtures in N₂. In the upper panel of Fig. 8, the QEPAS signal acquired for an unbalanced wet mixture containing 990 ppm CH₄ and 10 ppm C₂H₆:N₂ is displayed for an ICL current span from 20 mA to 70 mA at T = 15°C.

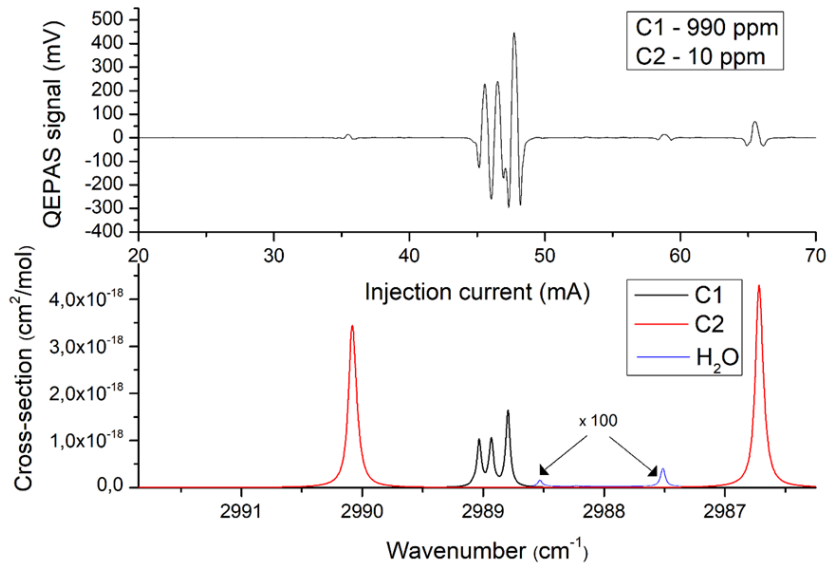


Figure 8. Top panel: QEPAS $2f$ -signal for a humidified mixture of 990 ppm-C1 and 10 ppm-C2:N₂ with an adjusted detection phase of ν_3^{C1} (φ_1) and ν_2^{C2} (φ_2). Bottom panel: absorption cross-section for C1 and C2 obtained using the Hitran database. Two weak H₂O peaks are also visible (blue curve), by multiplying the related cross-sections by a factor of 100.

The second derivative profile of ethane absorption features ν_1^{C2} , ν_2^{C2} and the second derivative shape of the three-lines structure from methane are clearly visible and the spectral separation is coherent with the absorption cross-section graph for both C1 and C2 simulated using the Hitran database and shown in the lower panel of Fig. 8.

While C1 and C2 are characterized by well-defined absorption peaks in the ICL operating range, propane shows a broadband absorption profile which merges with the C2 background signal in the ICL tuning range. Firstly, the sensor has been calibrated for C3 detection: the QEPAS spectra related to the C3 broadband spectra measured at atmospheric pressure and for different C3 dry concentrations, ranging from 1000 ppm to 200 ppm in pure N₂, were acquired. C2 and C3 calibration curves were used to set up a fitting procedure capable to retrieve both hydrocarbons concentration levels with high precision in wet C2/C3 mixtures in N₂.

In order to discriminate both contributions in C2/C3 mixtures, an injected current range from 35 to 60 mA was selected, in which range no strong C2 features are present and both C2 and C3 absorption broadband backgrounds can be easily compared (see Fig. 9a). As an example, it has been reported in Fig. 9 b) a balanced mixture of 500 ppm of C2 and 500 ppm of C3 in N₂.

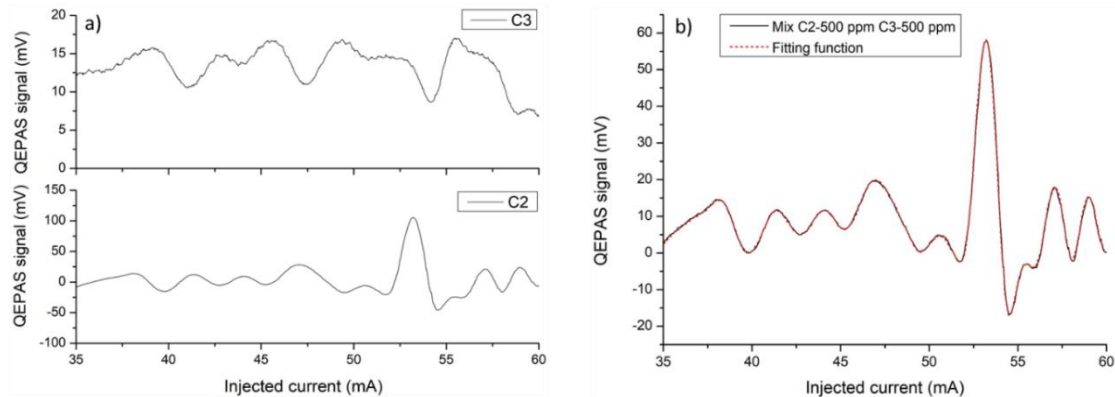


Figure 9 a) Top panel: $2f$ -signal for 1000 ppm-C3:N₂ acquired in the laser injected current range 35-60 mA. Bottom panel: $2f$ -signal for 1000 ppm-C2:N₂; b) $2f$ -signal for a dry mixture containing 500 ppm of C2 and 500 ppm of C3, in pure N₂.

By fitting the measured QEPAS signals with a MATLAB-based algorithm it is possible to extract the C2 and C3 concentration values. In Fig. 10 b) the QEPAS spectrum and the related fit are shown. Three different mixtures were analysed, and the calculated concentration values are listed in table II. In brackets the 95% confidence interval uncertainties are reported.

Table II: Actual and calculated C2 and C3 concentration for the investigated gas mixtures

Mixture	Actual C2 conc. (ppm)	Actual C3 conc. (ppm)	Calc. C2 conc. (ppm)	Calc. C3 conc. (ppm)
1	500	500	487.02 (± 1.4)	520.00 (± 2.5)
2	800	200	828.98 (± 3.8)	208.01 (± 6.8)
3	200	800	199.98 (± 1.7)	831.47 (± 2.9)

The small differences between the fitting parameters, i.e. the calculated C2, C3 concentrations and the extracted nominal concentrations remain below 5% and are mainly due to uncertainties in the certified gases flows used for producing the gas matrixes. The obtained results successfully demonstrate the feasibility to perform photoacoustic C2/C3 gas detection by fitting the QEPAS spectra measured for the gas mixtures.

Quartz-enhanced photoacoustic gas sensor employing a monolithic broadband distributed-feedback quantum cascade laser array

Many gaseous chemical compounds play a key-role in environmental monitoring, atmospheric science, and climate studies. Two such gases are nitrous oxide (N₂O) and methane (CH₄), both of which belong to a class of broadband absorbers, characterized by absorption bands wider than 50 cm⁻¹. The mid-infrared spectral range is particularly suitable for spectroscopy of broadband absorber gas spectroscopy. Among spectroscopic techniques, Quartz-Enhanced Photoacoustic Spectroscopy (QEPAS) has been demonstrated as one of the most efficient techniques for optical trace gas detection. Moreover, QEPAS employs a QTF as detector, whose responsivity is wavelength insensitive, and is thus particularly suitable for measurements over a broad spectral range.

A monolithic distributed-feedback quantum cascade laser array composed of 32 individual lasers fabricated on a single QCL chip has been employed as the light source for a QEPAS sensor, combining fast tuning speed over a wide spectral range with high stability. The broadband source

emits in pulsed mode from 1200 to 1310 cm^{-1} . The frequency spacing between consecutive QCL emitters is $\sim 4 \text{ cm}^{-1}$ and each one can be tuned of $\sim 3 \text{ cm}^{-1}$ by linearly varying the temperature from 15° C to 50 °C. The linewidth of each QCL emission is $\sim 1.5 \text{ cm}^{-1}$. In addition, the source operates in pulsed mode, allowing for low-power consumption.

The two broad spectral bands of nitrous oxide and several absorption lines of methane falling in the 1200 - 1310 cm^{-1} spectral range have been targeted for demonstration. Measurements were performed by switching the array QCLs in sequence while tuning their operating temperature to retrieve the fine structure of the two N_2O branches and the not equally separated absorption lines of CH_4 . In Fig. 10 a) and 10 b) we reported a comparison between the spectrum simulated using HITRAN database and the normalized QEPAS signals scaled to the normalized optical power, for a concentration of 1000ppm $\text{N}_2\text{O}:\text{N}_2$ and 1000ppm $\text{CH}_4:\text{N}_2$, respectively, while tuning the operating temperature of the QCL array.

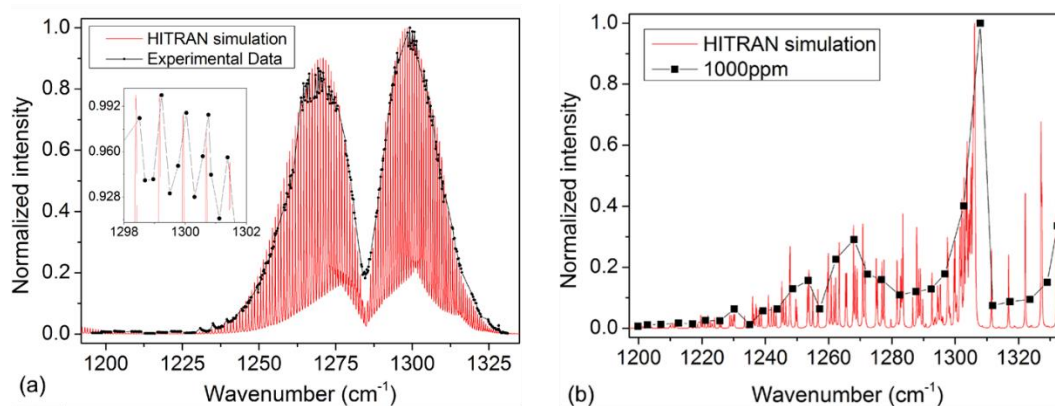


Fig. 10 Comparison between the normalized absorption spectra simulated using the HITRAN database (red solid lines) and the normalized signal collected for 1000ppm (black dots) of $\text{N}_2\text{O}:\text{N}_2$ (a) and $\text{CH}_4:\text{N}_2$ (b).

It can be observed that the acquired QEPAS signal well reproduces the two broad spectral bands of the N_2O . It is also possible to recognise some absorption structures of the CH_4 .

A sensor calibration was performed, demonstrating a linear responsivity for $\text{N}_2\text{O}:\text{N}_2$ and $\text{CH}_4:\text{N}_2$ concentrations from 1000 down to 200 parts-per-million. With a 10 seconds lock-in integration time a detection sensitivity of less than 60 parts-per-billion for N_2O and 190 parts-per-billion for CH_4 was achieved permitting the monitoring of nitrous oxide and methane at global atmospheric levels.

List of publications

- 1) P. Patimisco, A. Sampaolo, M. Giglio, V. Mackowiak, H. Rossmadl, B. Gross, A. Cable, F.K. Tittel, V. Spagnolo, Octupole electrode pattern for tuning forks vibrating at the first overtone mode in quartz-enhanced photoacoustic spectroscopy, *Optics Letters*, vol.43, issue 15 (2018)
- 2) A. Sampaolo, S. Csutak, P. Patimisco, M. Giglio, G. Menduni, V. Passaro, F.K. Tittel, M. Deffenbaugh, V. Spagnolo, Interband Cascade Laser Based Quartz-enhanced Photoacoustic Sensor for Multiple Hydrocarbons Detection, *Sensors and Actuators: B Chemical*, accepted (2018)
- 3) M. Giglio, P. Patimisco, A. Sampaolo, A. Zifarelli, R. Blanchard, C. Pfluegl, M. F. Witinski, D. Vakhshoori, F.K. Tittel, V. Spagnolo, Nitrous oxide quartz-enhanced photoacoustic detection employing a broadband distributed-feedback quantum cascade laser array, *Applied Physics Letters*, accepted (2018)

- 4) P. Patimisco, A. Sampaolo, M. Giglio, S. Dello Russo, V. Mackowiak, H. Rossmadl, A. Cable, F.K. Tittel, V. Spagnolo, Tuning forks with optimized geometries for quartz-enhanced photoacoustic spectroscopy, *Optics express*, submitted (2018)
- 5) M. Giglio, G. Menduni, P. Patimisco, A. Sampaolo, A. Elefante, V. Passaro, V. Spagnolo, Damping mechanisms of piezoelectric quartz tuning forks employed in photoacoustic spectroscopy for trace gas sensing, *Physica status solidi*, submitted (2018)

Conference Proceedings

- 1) V. Spagnolo, P. Patimisco, A. Sampaolo, M. Giglio, L. Dong, F.K. Tittel, Recent advances in quartz-enhanced photoacoustic sensing, *Journal Proceedings of SPIE - The International Society for Optical Engineering 10540-105402O* (2018)
- 2) A. Sampaolo, S. Csutak, P. Patimisco, M. Giglio, G. Menduni, V. Passaro, F.K. Tittel, M. Deffenbaugh, V. Spagnolo, Interband Cascade Laser Based Quartz-enhanced Photoacoustic Sensor for Multiple Hydrocarbons Detection, *Proceedings of SPIE - The International Society for Optical Engineering 10540-105400C* (2018)
- 3) P. Patimisco, A. Sampaolo, M. Giglio, F. Sgobba, H. Rossmadl, V. Mackowiak, B. Gross, A. Cable, F.K. Tittel, V. Spagnolo, Compact and Low-noise Quartz-enhanced Photoacoustic Sensor for Sub-ppm Ethylene Detection in Atmosphere, *Proceedings of SPIE - The International Society for Optical Engineering 10540-105401Q* (2018)
- 4) V. Spagnolo, P. Patimisco, A. Sampaolo, M. Giglio, V. Mackowiak, H. Rossmadl, B. Gross, A. Cable, F.K. Tittel, V. Spagnolo, New developments in quartz-enhanced photoacoustic spectroscopy for gas sensing applications, *Optics InfoBase Conference Paper, Volume Part F110-Sensors 2018* (2018)
- 5) M. Giglio, P. Patimisco, A. Sampaolo, P.P. Calabrese, J.M. Kriesel, F.K. Tittel, V. Spagnolo, Tapered Hollow-Core Fibers Providing Single-mode Output in the 3.5-7.8 μm spectral range, *Proceedings of SPIE - The International Society for Optical Engineering 10540-105402L* (2018)

Conference Talks

- 1) M. Giglio, P. Patimisco, A. Sampaolo, A. Elefante, F. Sgobba, F.K. Tittel, V. Spagnolo, Ethylene trace gas detection exploiting a compact quartz-enhanced photoacoustic spectroscopy-based sensor, *PIERS, 2018, Toyama, Japan*
- 2) M. Giglio, P. Patimisco, A. Sampaolo, J.M. Kriesel, F.K. Tittel, V. Spagnolo, Hollow-core waveguides for single mode delivery in the mid-infrared spectral range, (invited) *D-Photon 2018, Bari, Italy*

Teaching activities

- 1) Attività didattico-integrative per l'insegnamento "Fisica Generale" per la durata di 40 ore, Corsi Comuni – Politecnico di Bari, responsabile Prof. V. Spagnolo. Marzo 2018-Giugno 2018
- 2) Attività didattica relativa alla disciplina di FISICA nei corsi di preparazione e approfondimento per lo studio delle materie di base e del CAD per la durata di 8 ore – Politecnico di Bari. 13 settembre 2018 - 20 settembre 2018